Liu *et al. Chin. J. Mech. Eng.* (2018) 31:53
https://doi.org/10.1186/s10033-018-0255-0

Chinese Journal of Mechanical Engineering

ORIGINAL ARTICLE

Open Access

Experimental Investigation on Cooling/Heating Characteristics of Ultra-Thin Micro Heat Pipe for Electric Vehicle Battery Thermal Management

Fei-Fei Liu[1,2], Feng-Chong Lan[1], Ji-Qing Chen[1*] and Yi-Gang Li[1]

Abstract

Due to the heat pipes' transient conduction, phase change and fluid dynamics during cooling/heating with high frequency charging/discharging of batteries, it is crucial to investigate in depth the experimental dynamic thermal characteristics in such complex heat transfer processes for more accurate thermal analysis and design of a BTMS. In this paper, the use of ultra-thin micro heat pipe (UMHP) for thermal management of a lithium-ion battery pack in EVs is explored by experiments to reveal the cooling/heating characteristics of the UMHP pack. The cooling performance is evaluated under different constant discharging and transient heat inputs conditions. And the heating efficiency is assessed under several sub-zero temperatures through heating films with/without UMHPs. Results show that the proposed UMHP BTMS with forced convection can keep the maximum temperature of the pack below 40 °C under 1 ~ 3C discharging, and effectively reduced the instant temperature increases and minimize the temperature fluctuation of the pack during transient federal urban driving schedule (FUDS) road conditions. Experimental data also indicate that heating films stuck on the fins of UMHPs brought about adequate high heating efficiency comparing with that stuck on the surface of cells under the same heating power, but has more convenient maintenance and less cost for the BTMS. The experimental dynamic temperature characteristics of UMHP which is found to be a high-efficient and low-energy consumption cooling/heating method for BTMSs, can be performed to guide thermal analysis and optimization of heat pipe BTMSs.

Keywords: Electric vehicle, Lithium-ion battery, Thermal management, Ultra-thin micro heat pipe

1 Introduction

As a power source in an electric vehicle (EV) or an alternative in a hybrid electric vehicle (HEV) or a plug-in hybrid electric vehicle (PHEV), the power battery is adequately concerned by EV-manufacturers and users about its operation characteristics to meet the requirements of vehicles [1, 2]. For instance, perfect dynamic performance of charging/discharging to provide fast acceleration, long driving range, adequate motor assisting, idle-stop and regenerative braking, besides, good adaptability to work on the variable thermal environment (even extremely hot/cold) and excellent running safety [3–5]. Thus, the performance of the power battery system, including reliable operation, good cycle life, the accurate estimation of State of Charge (SOC) and State of Health (SOH), have determined the power, reliability, safety and cost of EVs [6, 7]. As a result, the issues caused by the above key factors will seriously affect the application of automobile.

Lithium-ion (Li-ion) power battery is considered to be a suitable candidate for EVs. In use, numbers of cells are connected to create a large battery module/pack in series/parallel. When working at high charge/discharge rate or severe thermal environment, large heat will be generated within cells, leading to rising temperature

*Correspondence: chjq@scut.edu.cn
[1] School of Mechanical & Automotive Engineering, Guangdong Key Laboratory of Automotive Engineering, South China University of Technology, Guangzhou 510641, China
Full list of author information is available at the end of the article

in the module/pack. Thus, the hotter cells decay faster, which shortens the lifespan of the module/pack [8]. Also, overheating and non-uniform temperature gradient without sufficient dissipation will deteriorate SOC and SOH of cells, which triggers the thermal runaway, premature failure of cells [9, 10]. Additionally, at low temperatures, a common phenomenon to Li-ion cells is that the capability and ageing will begin to deteriorate quickly as the temperature falls below −10 °C [11]. Thus, the optimal working temperature range of a Li-ion cell is 20–40 °C with less than 5 °C temperature gradient [12].

Among the reported researches [13–15] about different kinds of BTMSs for EVs, air, liquid, phase change material (PCM), cold plate and heat pipe have been considered and investigated. The above two methods or more were occasionally coupled to improve the heat transfer performance. Air is widely used because of its availability, convenient installation and low cost [16]. However, the non-uniform temperature still exists within large battery module/pack even using air forced [17]. Liquid usually has higher heat transfer coefficient and cooling/heating capacity than air. But more space, weight and energy consumption, possible leakage and complex maintenance are increased due to some extra facilities like pumps, valves, heat exchangers and tanks [18]. Phase change materials (PCMs) possess high thermal capacity of energy storage due to latent heat during phase changing [19, 20]. In fact, PCMs have no sufficient long term thermal stability because of their low thermal conductivity. Furthermore, the widespread use of PCMs in EVs is significantly limited by their use-cost and possible leakage by melting expansion.

Heat pipe, which is well known of its high-efficient phase change heat transfer, has recently been garnering more attention for high-efficient BTMSs. It not only possesses high thermal conductivity, compact and flexible structure, long lifetime and easy maintenance, but also has particular bidirectional characteristics (the evaporator and condenser can be switched according to actual cooling/heating needs) [21]. Rao et al. [22, 23] experimentally researched the cooling effect of a BTMS with oscillating heat pipe (OHP) for EVs. Tran et al. [24, 25] evaluated the thermal behavior of using tube heat pipes cooling for a HEV battery pack under natural/chimney convection and on several inclined positions. Greco et al. [26] analyzed the thermal performance of a BTMS by integrating tube heat pipes within a pipe set sandwiched with cells compared with that under forced convection. Ye et al. [27] carried out an experimental parametric study to assess the thermal characteristics of heat pipe cold plates (HPCPs) for Li-ion cell/pack with different charge rates and several cooling approaches.

To meet the requirements of limited space and lightweight of EVs, small sized heat pipe is more concerned for BTMS due to its extra advantages of more compact and lighter structure and more convenient installation. Zhao et al. [28] tested the cooling behavior of two BTMSs equipping different ultra-thin aluminum heat pipes for Li-ion packs, and concluded that heat pipe with wet cooling is the most effective solution to mitigate the temperature of cells. In Ref. [29], we have investigated the dynamic thermal characteristics of EV battery pack cooled by ultra-thin micro heat pipe (UMHP) via a "segmented" thermal resistance model with different convection and arrangement comparing with the test validation.

The above relevant researches revealed the excellent thermal performance of heat pipe BTMSs mainly based on the cooling effect at constant charge/discharge rate with different arrangements. As known, various heat transfer phenomena occur within a heat pipe, including transient conduction, phase change and fluid dynamics during cooling/heating with batteries' charging/discharging, which makes it difficult to obtain the full and real temperature variation characteristics in such complex heat transfer processes through theoretical analysis and calculation, especially using small sized heat pipes and/or under real driving conditions. In this case, for optimizing a BTMS, it is crucial to investigate in depth the experimental dynamic thermal performance for more accurate thermal analysis and design. So far, battery preheating through BTMS can be only found in limited researches [30, 31]. Recently, Wang et al. [32] provided a full experimental characterization forcing both cooling and heating of an "L" type heat pipe (flat on evaporator and tube on condenser) BTMS with liquid heat transfer on the condensers under "off-normal" operating conditions. Moreover, considering the miniaturization and compaction of the cooling/heating device to meet the requirements on optimal structure and arrangement in EVs, the advantage of heat pipes' bidirectional characteristic should be fully utilized for a well-design and high-efficient heat pipe BTMS to provide not only good cooling effect at high temperatures but also excellent preheating performance under low temperatures. In this paper, we explored the using of UMHP for both cooling and heating of a Li-ion battery pack in EVs. The experiments under different operation conditions are carried out to characterize the cooling/heating effects of the proposed UMHP BTMS. The main contributions of this work are developing such a small sized heat pipe and presenting its application to a BTMS with both cooling and heating, and then the experimental temperature characteristics of UMHPs can be performed to guide thermal analysis and optimization of heat pipe BTMSs.

This paper is organized as follows: Section 2 describes an UMHP BTMS for a Li-ion battery pack used in EVs; Section 3 presents an experimental set-up established for thermal evaluation of the UMHP pack; then the cooling performance of the UMHP pack is evaluated under constant discharging conditions and transient heat inputs on the federal urban driving schedule (FUDS) road condition, and two preheating methods by sticking heating films, 1) on the surface of cells and, 2) on the fins of UMHPs are compared to assess the heating efficiency under sub-zero temperatures in Section 4; finally, several conclusions are drawn in Section 5.

2 Description of UMHP BTMS

An initial design of an UMHP BTMS for a prismatic 3.2 V 50 Ah Li-ion battery pack with 5 cells in parallel in EVs is shown in Figure 1(a). In this pack, each cell is numbered from 1 to 5 along the y direction. Each UMHP with sintered copper–water is inserted into each cell cavity. The flat shape of UMHP is benefit to fit the prismatic surface of the cells for compact structure. The geometry of the cell and the arrangement of UMHP groups are shown in Figures 1(b)–(c). There are three groups of UMHPs with spacing s_{gp} in z direction. Each group consists of 4 UMHPs in parallel with spacing s_{hp} in y direction. The evaporator of each UMHP (i.e., l_{eva}) is directly contacted to the cell surface. For the cooling system, air convection is applied on the condenser of UMHP (i.e., l_{con}). Also, there are 6 pieces of aluminum fins fixed on each group condenser with spacing s_{fin} between two adjacent fins in x direction. For the heating system, two types of heating films, shown in Figure 1(d), are adopted to preheat the battery pack under sub-zero temperatures. There are 6 pieces of films of type 1 pasted to the surface of cells, and each cell is sandwiched between two films. Also, 18 pieces of films of type 2 are pasted to the fins of condensers. Each group has 6 pieces of films respectively staggered up and down on the fins in order to ensure the heating uniformity (presented in Figure 1(a)). The initial specifications of the UMHP pack are listed in Table 1.

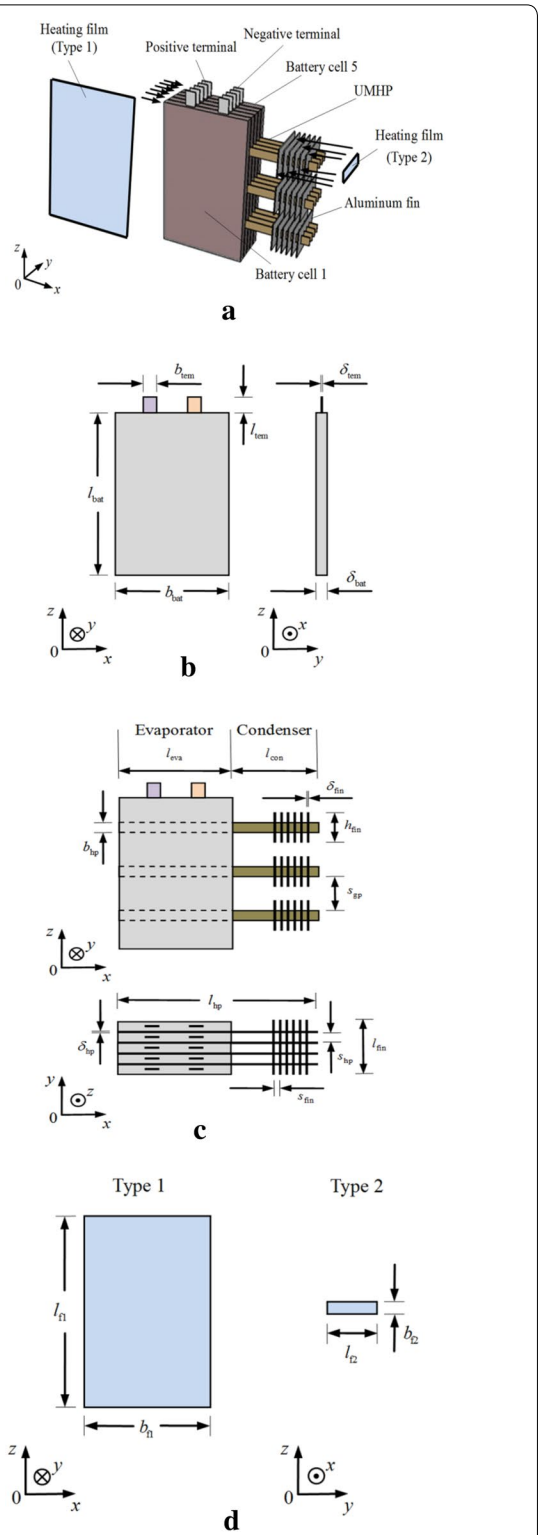

Figure 1 Demonstration of (**a**) the UMHP BTMS; (**b**) the battery cell; (**c**) the UMHP group and (**d**) the heating films

3 Experimental Set-up

The demonstration of test rig is shown in Figure 2. We took a prismatic Li-ion battery UMHP pack (3.2 V 50 Ah, 5 cells in parallel) as a sample for cooling/heating testing, shown in Figures 2(a)–(b). The arrangement of the UMHP pack is consistent with the initial model as shown in Figure 1(a). To keep good thermal conduction, a thermal conductive silicone is chosen to attach the UMHP groups to the cell surface. From Figure 2(a), for the cooling system, 3 helicoidal fans with dimension on 80×80 mm are fixed to blow air

Table 1 Initial specifications of the UMHP pack

Size	Initial value (mm)
Cell ($l_{bat} \times b_{bat} \times \delta_{bat}$)	155 × 102 × 10
Terminal ($l_{tem} \times b_{tem} \times \delta_{tem}$)	15 × 5 × 1
UMHP ($l_{hp} \times b_{hp} \times \delta_{hp}$)	168 × 10 × 1
Fin ($l_{fin} \times b_{fin} \times \delta_{fin}$)	55 × 35 × 0.5
Film of Type 1 ($l_{f1} \times b_{f1}$)	102 × 155
Film of Type 2 ($l_{f2} \times b_{f2}$)	55 × 12.5
s_{gp}	35
s_{hp}	10
s_{fin}	3

toward the condensers in parallel, and thus the cooling performance of the UMHP BTMS with air forced can be tested. From Figure 2(b), for the heating system, two types of heating films, i.e., 6 films of Type 1 (3.2 V 30 W/film) pasted to the surface of cells and 18 films of Type 2 (12 V 10 W/film) pasted to the fins of condensers, are adopted to preheat the pack under sub-zero temperatures. As presented in Figure 2(c), a Digatron battery test system (BTS-600) is used to charge/discharge for the UMHP pack with different rates. 20 K-type thermocouples (an uncertainty of ±1.5 °C) are arranged to obtain the detail temperature distribution of the UMHP pack, including 4 thermocouples on the surface cell, 10 embedded into the pack and 6 on the UMHPs, shown in Figure 2(d). A DHDAS dynamic signal analyzer is used to measure the temperatures at different locations of cells and UMHPs recorded by every ten seconds through the control computer. A programmable temperature chamber (an accuracy of ±0.5 °C, ranged from −70 to 150 °C) is used to regulate the testing temperature of the UMHP pack and to keep good thermal insulation. A power control is adopted to provide the required power of fans (or films) when cooling (or heating).

From Figure 2(d), the thermocouples are arranged from cell 1 to 3 due to the temperature symmetry in the pack. Among them, $T_{b1} \sim T_{b4}$, $T_{b5} \sim T_{b8}$ and $T_{b9} \sim T_{b14}$ are used to measure the temperatures of cells 1–3, respectively; $T_{p1} \sim T_{p3}$ and $T_{p4} \sim T_{p6}$ are used for evaporators and condensers of UMHPs respectively. Comparing with the tested temperatures, the maximum temperature of the pack and the temperature difference in pack/cell can be obtained.

In the testing, the chamber kept the UMHP pack at a working temperature (T_∞) of 30 °C during cooling and 0 °C/−10 °C/−20 °C under preheating. For cooling, firstly, the pack was charged at 0.5C rate from $S = 0.0$ to $S = 1.0$ with 3.65 ± 0.03 V cut-off voltage of charge, then the temperatures of the UMHPs and cells were tested respectively under 1 ~ 3C constant discharging until $S = 0.0$ with 2.5 V cut-off voltage of discharge. Also, the experiments on the cooling effect under transient FUDS road condition were carried out. For heating, two preheating methods by sticking heating films, 1) on the surface of cells and, 2) on the fins of UMHPs, were compared to predict the heating efficiency under sub-zero temperatures (0 °C/−10 °C/−20 °C). Each experimental condition was reproduced three times. For the temperature measurement at the same location of the UMHP pack, the deviation was no more than 1.5 °C. Therefore, the average tested temperature was presented in this paper.

4 Results and Discussions

The thermal performance of the UMHP pack are evaluated mainly using T_{max}, ΔT_{max}, $\Delta T_{max,pack}$ and ΔT_{hp}, where, T_{max}, the maximum temperature of the pack; ΔT_{max}, the maximum temperature rising between T_{max} and T_∞; $\Delta T_{max,pack}$, the difference between T_{max} and the minimum temperature of the pack; ΔT_{hp}, the temperature difference between evaporators and condensers.

4.1 Cooling of the UMHP pack

4.1.1 Tests under Constant Discharge Condition

As shown in Figure 3, the heat generation of cell (Q_{cell}) for tests under constant discharge rates (1 ~ 3C) vary with state of charge (S). Q_{cell} increases with the rising rate, especially obvious when $S < 0.2$, For 3C rate, Q_{cell} ranges from 3.58 W/cell to 4.98 W/cell. Consequently, the average heat generation of the UMHP pack at 1 ~ 3C was 2.22 W, 8.89 W and 20.01 W, respectively.

Figure 4 presents the temperature rising of the UMHP pack at 1 ~ 3C rates under natural/forced convections. ΔT_{max} and $\Delta T_{max,pack}$ increase obviously at high rates and $S < 0.4$. For natural convection, ΔT_{max} is as high as 13.5 °C and 20.4 °C, and $\Delta T_{max,pack}$ can be up to 5.5 °C and 6.1 °C at the end of 2 ~ 3C discharging respectively, which can not satisfy the dissipation requirements of the cells. For the forced convection, the air flow speed (v) at the outside of fins was 6±0.8 m/s; ΔT_{max} is 5.6 °C, 7.0 °C and 10.4 °C lower and $\Delta T_{max,pack}$ is 2.6 °C, 2.8 °C and 3.0 °C lower than that with natural convection at 1 ~ 3C rates, respectively. The uniformity of temperature in the pack is improved by UMHPs with air forced, which has higher heat transfer coefficient and can efficiently dissipate more heat generated by the pack compared to that with natural convection.

Figure 5 shows the temperature of the UMHPs (T_{hp}) under natural/forced convection at 3C rate. As present, the temperature of evaporator (T_e) is higher than that of condenser (T_c); among the three UMHP groups, the temperatures of group 1 are the highest, then followed by group 3, and the values of group 2 are the lowest; but

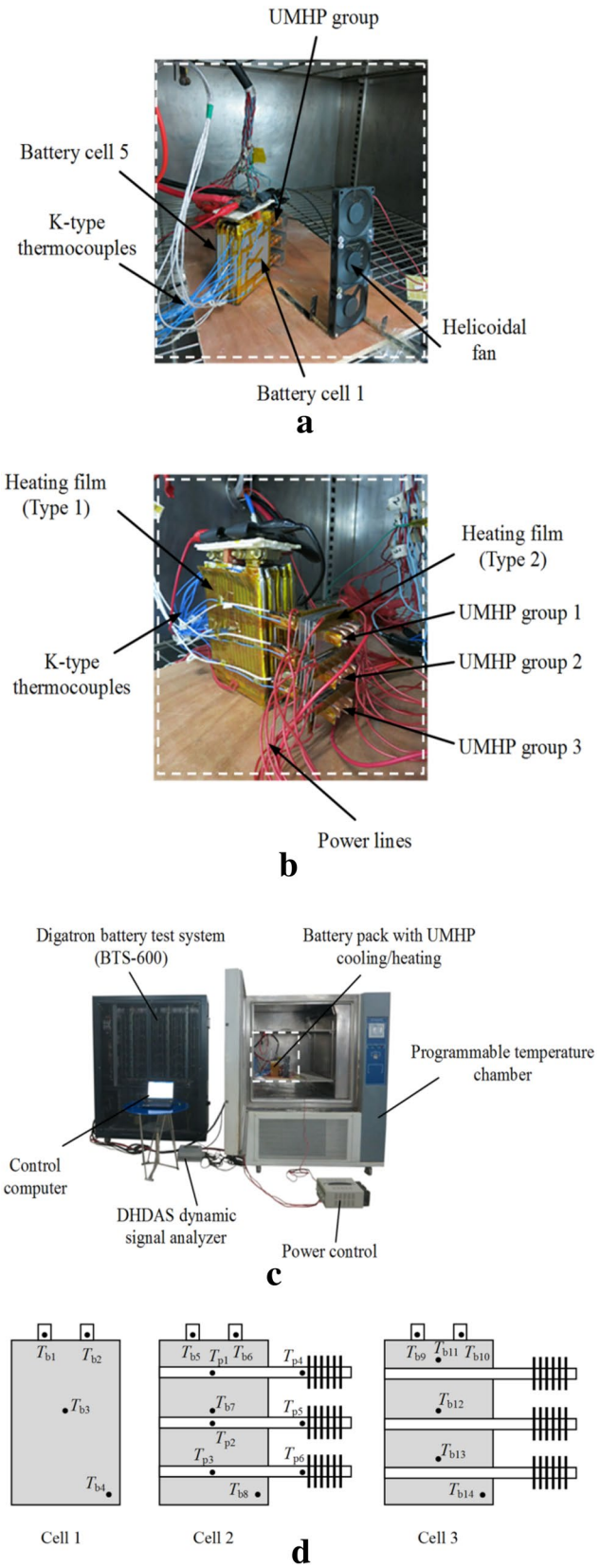

Figure 2 Demonstration of testing: (**a**) UMHP cooling; (**b**) UMHP heating; (**c**) test rig and (**d**) arrangement of thermocouples on the UMHP pack

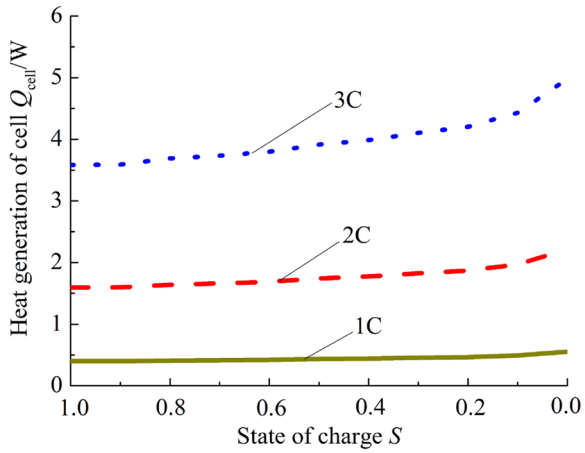

Figure 3 Heat generation of cell (Q_{cell}) for tests under 1 ~ 3C constant discharge

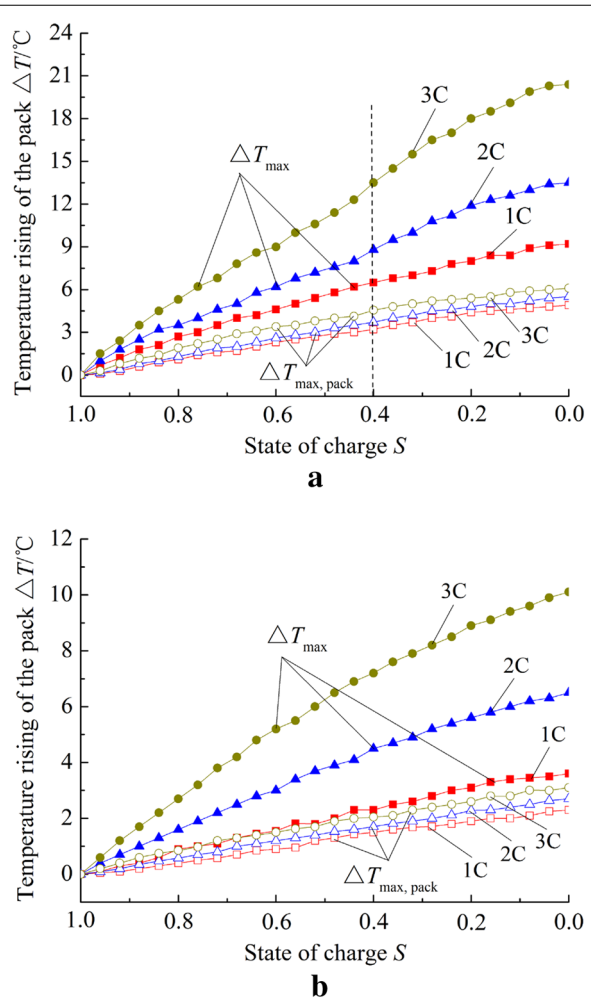

Figure 4 Temperature rising of the UMHP pack under (**a**) natural and (**b**) forced convection at 1 ~ 3C rates

the maximum temperature difference between evaporators (or condensers) is less than 2 °C. Also, a small delay (flat line) from the initial temperature of condensers can be found. Under natural convection, presented in Figure 5(a), this delay continues to $S = 0.90$. Then T_e and T_c gradually increase almost in parallel trend. However, ΔT_{hp} becomes increasing when $S < 0.40$, the value is up to 6.4 °C at the end of discharge. This can be attributed to that the working medium in the evaporators evaporates too quickly, but there is no rapid dissipation on the condensers. This causes the working medium in the evaporator insufficient supplement, and the drying up phenomenon may appear in UMHPs, thus results in insufficient dissipation.

From Figure 5(b), the above delay is somewhat shortened under the forced convection, temperature increase appears on $S = 0.94$ for condensers. This indicates that the UMHP needs a certain temperature difference (no less than 1.0 °C) between T_e and T_c to start work. Due to the surface heat transfer coefficient of condensers increased by the influence of air flow under forced convection, the start working time can be reduced about 48 s, and the working medium in evaporators can work continuously to transfer the heat generated by cells to the condensers. ΔT_{hp} increases gradually until 4.7 °C at the ending of discharge. All the test results indicate that UMHP cooling combined with forced convection is found to be a preferred solution to improve the dissipation of BTMSs.

4.1.2 Tests under Transient Condition

For EVs, there exist complex road conditions during operation, including quick acceleration/deceleration, good grade ability and so on. Taking FUDS road condition ($T_\infty = 30 \pm 1.5$ °C) for experiments, the electric current (I) and heat generation (Q) of the UMHP pack versus the charge/discharge time (3600 s) are presented in Figure 6. Unlike the constant discharge, the charge/discharge processing of the practical operation condition is varying with the cells' heat generation of large amplitude and high frequency. The maximum charge and discharge rate can be up to 1.5C and 3.3C respectively, leading to the maximum heat generation as high as 130 W.

The temperature variations of the cells and UMHPs with air forced convection ($v = 6$ m/s) under the FUDS condition are shown in Figure 7. From Figure 7(a), the cells' temperatures with/without UMHPs increase gradually and fluctuate with the cells' heat generation. At the beginning 300 s, the increasing value of $T_{max}(T_{b9})$ is up to 8.5 °C without UMHPs, but only 3.4 °C with UMHPs. The maximum temperatures of different measurements all appear at about 3000 s, $T_{max}(T_{b9})$ and $\Delta T_{max,pack}$ ($T_{b9} - T_{b4}$) with UMHP cooling are 39.1 °C and 3.6 °C,

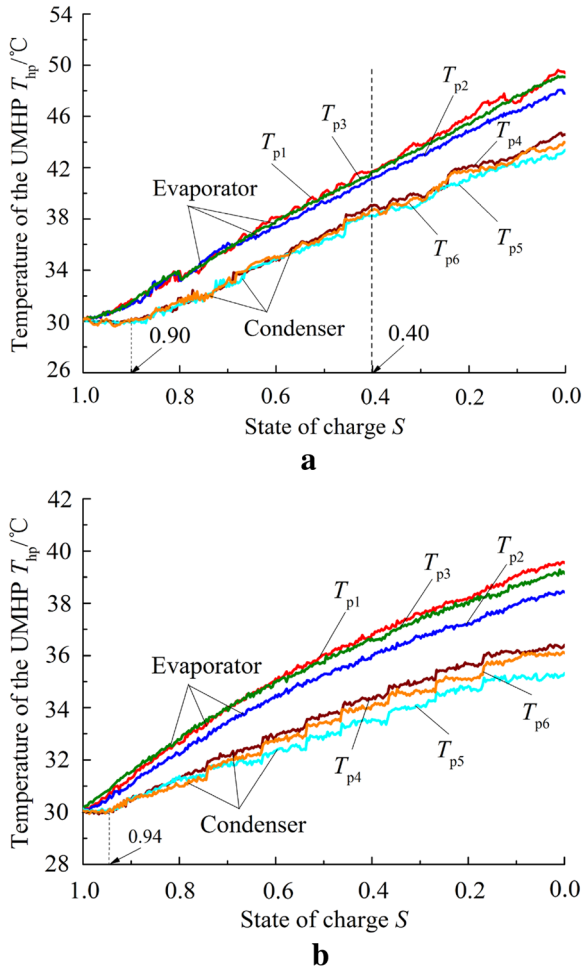

Figure 5 Temperature of the UMHPs under (**a**) natural and (**b**) forced convection at 3C discharge

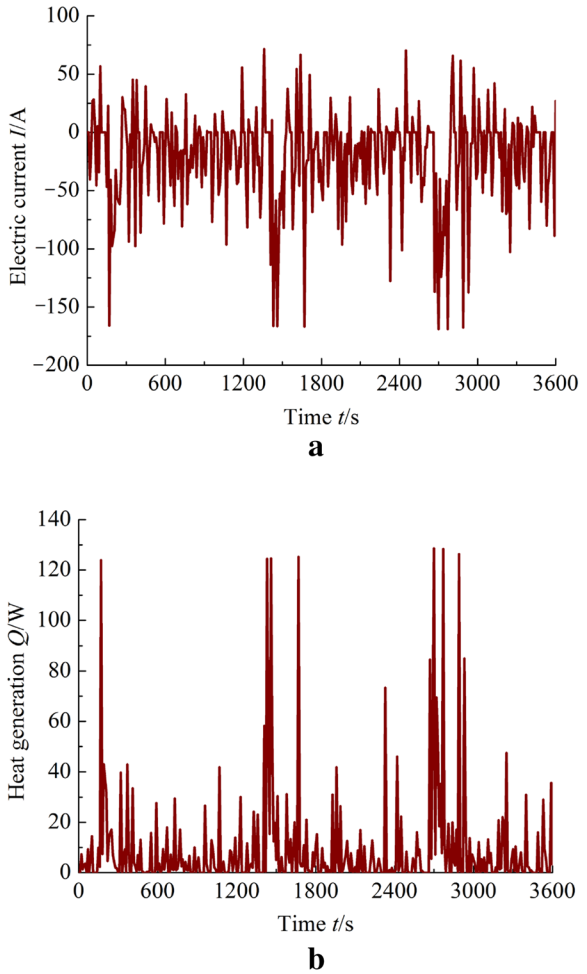

Figure 6 Variations of (**a**) electric current and (**b**) heat generation of the UMHP pack

respectively by 13.5 °C and 1.8 °C lower than that without UMHPs.

From Figure 7(b), the temperature rising trends of the evaporators are similar to that of cells due to their direct contact. For the condensers, there exists about 100 s delay in temperature rising from start time, here, ΔT_{hp} is about 1.2 °C. The temperatures fluctuate with the amplitude of 1.5 °C for the condensers, but 2.2 °C for the evaporators. ΔT_{hp} is gradually increased with the maximum value less than 5.5 °C at the end of time. All the test results indicate that adding UMHPs to the battery pack can effectively reduce instant temperature increases caused by battery's high-frequency heat generation and minimize the temperature fluctuation during transient FUDS conditions.

4.2 Heating of the UMHP Pack

The heat source can be obtained through heating films from electric power to preheat the battery pack under low temperatures. In this work, two preheating methods: 1) sticking 6 pieces of heating films of Type 1 on the surface of cells and 2) sticking 18 pieces of heating films of Type 2 on the fins of UMHPs, were used to compare the heating efficiency under sub-zero temperatures. For the former, the heat from each film is directly transferred to the contacted surface of cells; for the latter, the heat is transferred through fins to the UMHPs and then to the cells by utilizing the advantage of heat pipes' bidirectional characteristics. The UMHP pack was respectively set during cold exposure under 0 °C/−10 °C/−20 °C for more than 8 h in the programmable temperature chamber before experiments.

From Figure 8, preheating cells with Method 1 was more efficient comparing with Method 2 at the beginning of heating. For the Method 2, a small delay (flat line) in temperature increase from the initial sub-zero temperatures can be observed, about 38 s for cell 3 and 100 s for

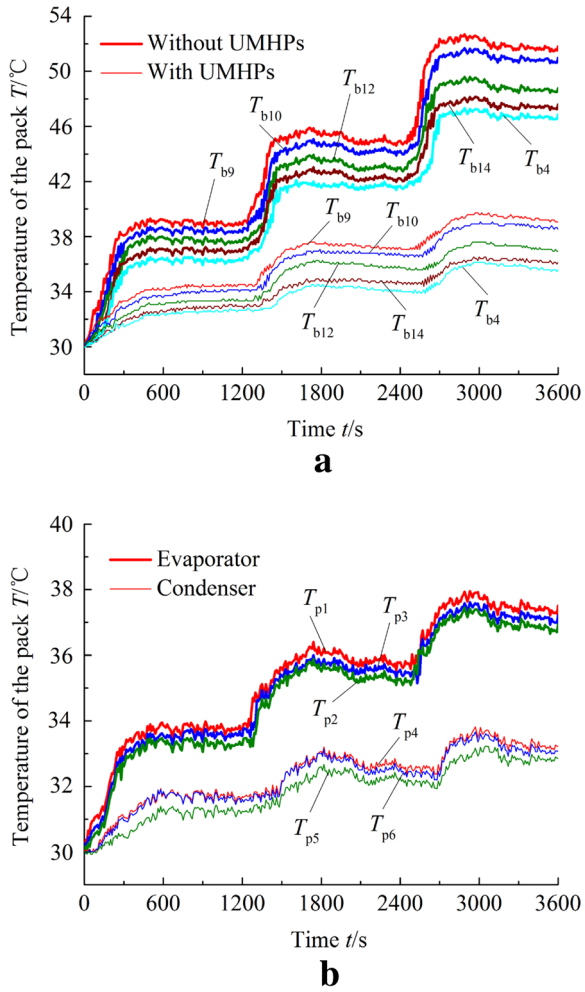

Figure 7 Temperature variation of (**a**) the cells and (**b**) the UMHPs with air forced convection under the FUDS condition

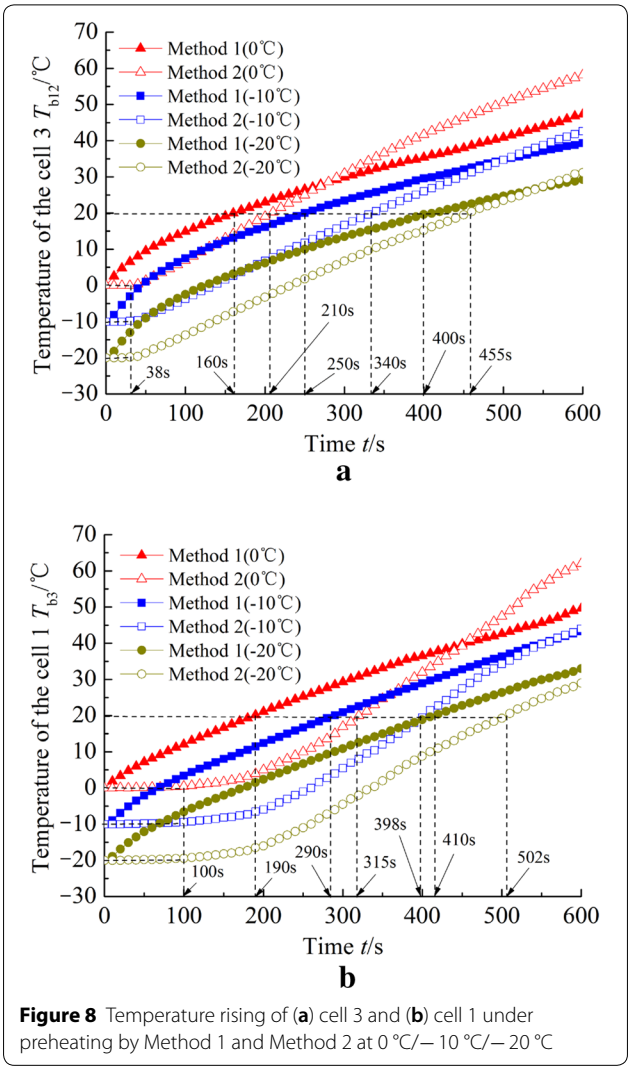

Figure 8 Temperature rising of (**a**) cell 3 and (**b**) cell 1 under preheating by Method 1 and Method 2 at 0 °C/− 10 °C/− 20 °C

cell 1. Then, the rates of temperature rising with Method 2 were higher than that with Method 1. In order to heat the cells from 0 °C/− 10 °C/− 20 °C to 20 °C, about 160 s/250 s/400 s for cell 3 and 190 s/290 s/410 s for cell 1 were required with Method 1 and approximately 210 s/340 s/455 s and 315 s/398 s/502 s with Method 2, respectively. This indicated that the heating efficiency by preheating cells with Method 1 is slightly higher (no more than 125 s) than that with Method 2 under the same heating power (a total of 180 W).

Figure 9 compares the temperature increase of the UMHPs by the two preheating methods at − 10 °C. For Method 1, the heating films were directly stuck on the surface of cells; the heat from films could be conducted to the evaporators immediately. This caused T_e of each group almost linear increase by about 10 °C higher than that of condensers after 50 s. When T_e was reached 20 °C, more than 255 s was needed. However, for the heat pipe alone, a small delay in temperature increase of condensers appeared, and lasted about 20 s. For Method 2, the heat from heating films was transferred through fins to the condensers. As a result, T_c showed a sharp rising in the first 80 s, the average increasing rate could be up to 1 °C/s; then flattened at about 80 °C. However, T_e of each group increased linearly after 30 s time delay from the beginning of preheating, and were up to 20 °C when preheating for approximately 325 s. Moreover, all the results showed that UMHPs were able to operate effectively even after long hours of cold exposure without losing its complete function.

Compared with the two preheating methods, the time when T_e reached 20 °C from − 10 °C with Method 1 was about 35 s less than that with Method 2. This was not great advantage for the Method 1 because this needed larger size heating films, the heat transfer surface of which were about 7.7 times more than that with Method

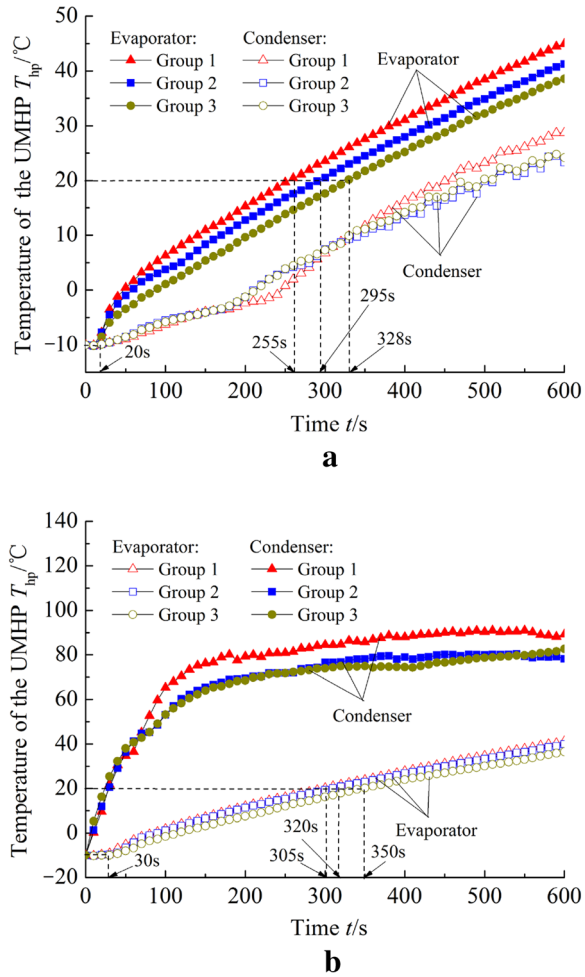

Figure 9 Temperature rising of the UMHPs under preheating by (**a**) Method 1 and (**b**) Method 2 at −10 °C

2 under the same heating power, which will cause more cost of BTMSs. Moreover, Method 1 increases more difficulties of maintenance than Method 2 when the cells are integrated in a package for EV applications.

5 Conclusions

(1) Considering the limited space allocated for the battery pack and lightweight of EVs, UMHP is found to be a high-efficient and low-energy consumption method for BTMSs.

(2) Adding UMHPs can improve the dissipation performance under different constant discharge rates. Consequently, T_{max} and $\Delta T_{max,pack}$ are kept below 40 °C and 5 °C, respectively under 1 ~ 3C discharging with forced convection ($v = 6$ m/s).

(3) With high frequency and large amplitude variable heat generation, adding UMHPs to the battery pack can effectively reduce the instant temperature increases and minimize the temperature fluctuation during transient FUDS conditions.

(4) Sticking heating films on the fins of UMHPs has adequate high heating efficiency (no more than 125 s) comparing to sticking on the surface of cells under the same heating power when preheating from sub-zero temperatures (0 °C/−10 °C/−20 °C) to 20 °C. But the former is much more cost-efficient for BTMS with heating films by smaller size and more convenient maintenance.

In the following work,the heat pipe system combined with PCMs may be taken into account to strengthen the cooling/heating effect for BTMSs. Because of the complicated fabrication process and the use of copper as the wall and wick material, the cost of heat pipe limits its wide application in BTMS. Therefore, considering the aluminum heat pipe manufacturing and feasibility [33, 34], the investigation on applying aluminum heat pipe in BTMS can be revealed as effective and reliable way to reduce the cost and weight of EV. In order to validate the use of UMHP in EV application, the thermal performance of UMHP BTMS by considering the influence of EV shock and vibration can be investigated in the future.

Authors' Contributions
F-CL and J-QC were in charge of the whole trial; F-FL wrote the manuscript; Y-GL assisted with sampling and laboratory analyses. All authors read and approved the final manuscript.

Author details
[1] School of Mechanical & Automotive Engineering, Guangdong Key Laboratory of Automotive Engineering, South China University of Technology, Guangzhou 510641, China. [2] School of Mechatronics & Vehicle Engineering, East China Jiaotong University, Nanchang 330013, China.

Authors' Information
Fei-Fei Liu, born in 1983, is currently a lecturer at *School of Mechatronics & Vehicle Engineering, East China Jiaotong University, China*. She received her PhD degree from *South China University of Technology, China*, in 2017. Her research interests include automotive thermal environment adaptability and thermal management research.

Feng-Chong Lan, born in 1959, is currently a professor and a PhD candidate supervisor at *School of Mechanical & Automotive Engineering, South China University of Technology, China*. He received his PhD degree from *Jilin University, China*, in 1998. His research interests include automotive body structure and safety and automotive occupant's thermal comfort performance.

Ji-Qing Chen, born in 1966, is currently a professor and a PhD candidate supervisor at *School of Mechanical & Automotive Engineering, South China University of Technology, China*. She received her two PhD degree from *Salford University, UK*, 2005 and *Jilin University, China*, in 1998. Her research interests include lightweight and crashworthiness design of car body structure, simulation and theory of occupant's thermal comfort.

Yi-Gang Li, born in 1989, is currently a PhD candidate at *School of Mechanical & Automotive Engineering, South China University of Technology, China*. He received his Master degree from *Central South University, China*, in 2013. His research interests include system modeling and simulation for EV and the application of modern control theory in EV control system.

Competing Interests
The authors declare no competing financial interests.

Ethics Approval and Consent to Participate
Not applicable.

Funding
Supported by National Natural Science Foundation of China (Grant No. 51775193), Guangdong Provincial Science and Technology Planning Project of China (Grant Nos. 2014B010125001, 2014B010106002, 2016A050503021), and Guangzhou Municipal Science and Technology Planning Project of China (Grant No. 201707020045).

Publisher's Note

Received: 25 September 2016 Accepted: 13 June 2018
Published online: 26 June 2018

References

1. Dong-Ye Sun, Xin-You Lin, Da-Tong Qin, et al. Power-balancing instantaneous optimization energy management for a novel series-parallel hybrid electric bus. *Chinese Journal of Mechanical Engineering*, 2012, 25(6): 1161-1170.
2. Wei-Da Wang, Li-Jin Han, Chang-Le Xiang, et al. Synthetical Efficiency-based optimization for the power distribution of power-split hybrid electric vehicles. *Chinese Journal of Mechanical Engineering*, 2014, 27(1): 58-68.
3. S Amjad, S Neelakrishnan, R Rudramoorthy. Review of design considerations and technological challenges for successful development and deployment of plug-in hybrid electric vehicles. *Renewable and Sustainable Energy Reviews*, 2010, 14(3): 1104-1110.
4. Da-Xu Sun, Feng-Chong Lan, Yun-Jiao Zhou, et al. Control algorithm of electric vehicle in coasting mode based on driving feeling. *Chinese Journal of Mechanical Engineering*, 2015, 28(3): 479-486.
5. Ya-Lian Yang, Xiao-Song Hu, Huan-Xin Pei, et al. Comparison of power-split and parallel hybrid powertrain architectures with a single electric machine: Dynamic programming approach. *Applied Energy*, 2016, 168: 683-690.
6. Yuan Zou, Xiao-Song Hu, Hong-Min Ma, et al. Combined state of charge and state of health estimation over lithium-ion battery cell cycle lifespan for electric vehicles. *Journal of Power Sources*, 2015, 273: 793-803.
7. R Mahamud, C Park. Reciprocating air flow for Li-ion battery thermal management to improve temperature uniformity. *Journal of Power Sources*, 2011, 196(13): 5685-5696.
8. Fei-Fei Liu, Feng-Chong Lan, Ji-Qing Chen. Simulation and experiment on temperature field of lithium-ion power battery for vehicle based on characteristic of dynamic heat source. *Journal of Mechanical Engineering*, 2016, 52(8): 141-151. (in Chinese)
9. Y Troxler, B Wu, M Marinescu, et al. The effect of thermal gradients on the performance of lithium-ion batteries. *Journal of Power Sources*, 2014, 247: 1018-1025.
10. Zhe Li, Xue-Bing Han, Lan-Guang Lu, et al. Temperature characteristics of power $LiFePO_4$ batteries. *Journal of Mechanical Engineering*, 2011, 47(18): 115-120. (in Chinese)
11. T Waldmann, M Wilka, M Kasper, et al. Temperature dependent ageing mechanisms in Lithium-ion batteries—A Post-Mortem study. *Journal of Power Sources*, 2014, 262: 129-135.
12. Tao Wang, K J Tseng, Ji-Yun Zhao, et al. Thermal investigation of lithium-ion battery module with different cell arrangement structures and forced air-cooling strategies. *Applied Energy*, 2014, 134: 229-238.
13. Zhong-Hao Rao, Shuang-Feng Wang. A review of power battery thermal energy management. *Renewable and Sustainable Energy Reviews*, 2011, 15(9): 4554-4571.
14. X M Xu, R He. Review on the heat dissipation performance of battery pack with different structures and operation conditions. *Renewable and Sustainable Energy Reviews*, 2014, 29: 301-315.
15. H Park. A design of air flow configuration for cooling lithium ion battery in hybrid electric vehicles. *Journal of Power Sources*, 2013, 239: 30-36.
16. X M Xu, R He. Research on the heat dissipation performance of battery pack based on forced air cooling. *Journal of Power Sources*, 2013, 240: 33-41.
17. Li-Wu Fan, J M Khodadadi, A A Pesaran. A parametric study on thermal management of an air-cooled lithium-ion battery module for plug-in hybrid electric vehicles. *Journal of Power Sources*, 2013, 238: 301-312.
18. Kai-Wei Chen, Xian-Guo Li. Accurate determination of battery discharge characteristics—A comparison between two battery temperature control methods. *Journal of Power Sources*, 2014, 247: 961-966.
19. Zi-Ye Ling, Jia-Jie Chen, Xiao-Ming Fang, et al. Experimental and numerical investigation of the application of phase change materials in a simulative power batteries thermal management system. *Applied Energy*, 2014, 121: 104-113.
20. F Samimi, A Babapoor, M Azizi, et al. Thermal management analysis of a Li-ion battery cell using phase change material loaded with carbon fibers. *Energy*, 2016, 96: 355-371.
21. X Yang, Y Y Yan, D Mullen. Recent developments of lightweight, high performance heat pipes. *Applied Thermal Engineering*, 2012, 33-34: 1-14.
22. Zhong-Hao Rao, Shuang-Feng Wang, Mao-Chun Wu, et al. Experimental investigation on thermal management of electric vehicle battery with heat pipe. *Energy Conversion and Management*, 2013, 65: 92-97.
23. Zhong-Hao Rao, Yu-Tao Huo, Xin-Jian Liu. Experimental study of an OHP-cooled thermal management system for electric vehicle power battery. *Experimental Thermal and Fluid Science*, 2014, 57: 20-26.
24. T Tran, S Harmand, B Sahut. Experimental investigation on heat pipe cooling for Hybrid Electric Vehicle and Electric Vehicle lithium-ion battery. *Journal of Power Sources*, 2014, 265: 262-272.
25. T Tran, S Harmand, B Desmet, et al. Experimental investigation on the feasibility of heat pipe cooling for HEV/EV lithium-ion battery. *Applied Thermal Engineering*, 2014, 63(2): 551-558.
26. Angelo Greco, Dong-Pu Cao, Xi Jiang, et al. A theoretical and computational study of lithium-ion battery thermal management for electric vehicles using heat pipes. *Journal of Power Sources*, 2014, 257: 344-355.
27. Yong-Huang Ye, Yi-Xiang Shi, Saw Liphuat, et al. Performance assessment and optimization of a heat pipe thermal management system for fast charging lithium ion battery packs. *International Journal of Heat and Mass Transfer*, 2016, 92: 893-903.
28. Rui Zhao, Jun-Jie Gu, Jie Liu. An experimental study of heat pipe thermal management system with wet cooling method for lithium ion batteries. *Journal of Power Sources*, 2015, 273: 1089-1097.
29. Feifei Liu, Fengchong Lan, Jiqing Chen. Dynamic thermal characteristics of heat pipe via segmented thermal resistance model for electric vehicle battery cooling. *Journal of Power Sources*, 2016, 321: 57-70.
30. P Nelson, D Dees, K Amine, et al. Modeling thermal management of lithium-ion PNGV batteries. *Journal of Power Sources*, 2002, 110(2): 349-356.
31. X Duan, G F Naterer. Heat transfer in phase change materials for thermal management of electric vehicle battery modules. *International Journal of Heat and Mass Transfer*, 2010, 53(23-24): 5176-5182.
32. Q Wang, B Jiang, Q F Xue, et al. Experimental investigation on EV battery cooling and heating by heat pipes. *Applied Thermal Engineering*, 2015, 88: 54-60.
33. Y T Chen, S W Kang, Y H Hung, et al. Feasibility study of an aluminum vapor chamber with radial grooved and sintered powders wick structures. *Applied Thermal Engineering*, 2013, 51: 864-870.
34. M Ameli, B Agnewa, P S Leung, et al. A novel method for manufacturing sintered aluminium heat pipes (SAHP). *Applied Thermal Engineering*, 2013, 52: 498-504.